Available online at www.sciencedirect.com
SCIENCE DIRECT®
Electrochimica Acta 50 (2005) 3033–3039
ELECTROCHIMICA Acta
www.elsevier.com/locate/electacta

Electrochemical production of nanopore arrays in a nickel aluminium alloy

Achim Walter Hassel *,[1], Belen Bello-Rodriguez, Srdjan Milenkovic, André Schneider

Max-Planck-Institut für Eisenforschung, Max-Planck-Str. 1, D-40237 Düsseldorf, Germany

Received 20 September 2004; received in revised form 23 December 2004; accepted 25 December 2004

Abstract

Directional solidification of a eutectic is a novel route for the production of nanostructures. This method was applied to the quasibinary NiAl–Re system. Re as the minor phase forms fibers, which are parallel aligned in the NiAl matrix. At a temperature of $1690 \pm 10\,^{\circ}C$ using a thermal gradient of $40\,^{\circ}C\,cm^{-1}$ and a growth rate of $30\,mm\,h^{-1}$, the fibers formed had a diameter of about 400 nm. An electrochemical method is presented here that simultaneously passivates the NiAl matrix and selectively electrodissolves the Re. In this manner, it was possible to form an array of nanopores each with the same diameter of 400 nm. The mechanisms behind this procedure, as well as the potential of this method for the production of nanoelectrode arrays or nanofilters are discussed.

Keywords: Nanotechnology; Nanopores; Nanoelectrode; Nanofilter; Electrochemical nanosystem technology

1. Introduction

It is commonly accepted that nanotechnology is an enabling technology and will without doubt be one of the key technologies in the next decades. All kinds of nanostructures are presently under investigation. Nanowires and nanotubes are of special interest as they are one-dimensional objects that can carry a function on one side and inherently provide a proper connection [1,2]. Carbon nanowires and carbon nanotubes are the most investigated objects [3]. The preparation of metallic or semiconductor wires requires different techniques [4,5]. Semiconductor wires are mostly grown from the gas phase. Metallic wires can be grown for instance electrochemically by deposition into templates of porous alumina. This porous alumina as well as the here introduced metal wire arrays are self organised nanostructures (SONS). This self organisation is generally an advantage as on one hand, it allows the production of systems with an inherent order and on the other, can be alternatively used for the simultaneous production of a large number of identical or at least similar nanoobjects.

Directional solidification is a method that allows the production of nanowire arrays or nanobelt systems [6]. It may sound contradictory to apply a method that was developed to produce large single crystals to generate nanostructures. This method is commonly used to produce high strength materials for the application at high temperatures such as turbine blades. Here, it is introduced how such a nanostructured material can be processed to form an array of nanopores. This technique has the potential for the production of either nanoelectrode arrays of noble metals for the employment in sensors or for the production of nanofilter systems for sterile filtration or gas cleaning.

2. Experimental

2.1. Materials and chemicals

As a starting material, nickel (99.97 wt.%), electrolytic aluminium (99.9999 wt.%) and rhenium pellets (99.9 wt.%) were used for the alloy preparation. Pre-alloys were prepared

* Corresponding author. Fax: +49 211 6792 218.
E-mail address: hassel@elchem.de (A.W. Hassel).
[1] ISE active member.

0013-4686/$ – see front matter © 2005 Elsevier Ltd. All rights reserved.
doi:10.1016/j.electacta.2004.12.046

by induction melting under inert atmosphere and drop casting into a cylindrical copper mould. The eutectic alloy contains 5.5% (w/w) Re which was confirmed by a chemical analysis (Section 3.2)

All solutions were prepared from p.a. grade chemicals and high purity water (Millipore filter system). A 1 M acetate buffer of pH 6.0 was used for all experiments. All materials used were of analytical grade and purchased by Merck (Darmstadt, Germany).

2.2. Directional solidification

Subsequently, the as cast ingots were machined to fit into alumina crucibles and directionally solidified in a Bridgman type crystal growing facility. It consists of the crucible support, cooling ring and heating element (tungsten net). The alumina crucible with the as cast ingot was positioned in the furnace and heated up to ∼1700 °C. After the material in the crucible was completely melted, the upper part with the heating element is slowly and uniformly shifted upwards, providing thus unidirectional heat extraction. This operation is controlled by a servomotor that enables speed range from 1 to 200 mmh. The experiments were conducted at the temperature of 1690 ± 10 °C, thermal gradient of approximately 40 °C cm^{-1} and growth rate of 30 mm h^{-1}.

2.3. Chemical dissolution

The extraction of Re nanofibers from the NiAl–Re eutectic alloy was accomplished by selectively etching the NiAl matrix. The selective etching of the NiAl phase in the alloy was achieved after digestion of the sample into a solution containing 3.2% HCl and 3% H_2O_2 in distilled water. The eutectic alloy was cut in 1 cm × 1 cm × 1 cm cubes, which were then immersed into the HCl/H_2O_2 mixture and left stirring overnight. The green solution obtained with this treatment was afterwards filtered using a glass vacuum filter unit with 0.2 μm pore size cellulose acetate membranes (Sartorius, Göttingen, Germany). Analysis of the filtered solution and membrane was performed by inductively coupled plasma optical emission spectroscopy (ICP-OES) in order to calculate the total content of the three metals of interest Ni, Al and Re. Independent calibration curves were used for each of the elements to guarantee an independent quantification. As a result, the sum can deviate from 100.0%.

2.4. Electrochemical equipment

For selective electrochemical dissolution of the rhenium fibers, a conventional three-compartment cell with working, reference and counter electrodes was employed. The volume of the cell compartment was 20 ml. The fabricated NiAl–Re alloy was cut in 1 cm thick cubes and mechanically mirror-like ground and polished prior to measurements. These samples could be embedded or fixed in a specially designed Teflon sample holder to expose exactly 1 cm^2 to the electrolyte. Its potential as working electrode was measured with respect to a commercial Ag/AgCl (Metrohm, Filderstadt, Germany). A smooth Au foil electrode was employed as counter (apparent surface area = 2 cm^2). A PST050 potentiostat (Radiometer Analytical, Lyon, France) was used in all electrochemical measurements. Measurements were performed at room temperature in non-deaerated and quiescent solutions of 1 M acetate buffer (pH 6.0).

2.5. Electron microscopy

Scanning electron microscopy pictures were obtained on a high resolution scanning electron microscope with field emission gun (Leo 1550 VP apparatus Leo Elektronenmikroskopie GmbH, Oberkochem, Germany) fitted with an INCA energy dispersive system (EDS) (Oxford Instruments, Oxford, UK).

3. Results and discussion

3.1. Eutectic growth

During eutectic reaction, a liquid phase transforms in two or more solid phases at unique temperature and composition, which makes it an invariant reaction. The peculiarity is that the forming phases solidify simultaneously despite having quite different compositions. This reaction is schematically shown in Fig. 1. Component B is rejected by the growing α-phase, while A is rejected by the β-phase. This leads to a concentration built-up of components A and B ahead of β- and α-phase, respectively. Hence, a concentration gradient along the solidification front is established, which force A and B atoms to diffuse laterally to the growth interface, i.e. the growth is coupled by the diffusion field in front of the growing interface. This growth mechanism is denoted cooperative or coupled growth.

The microstructures of binary eutectic alloys can exhibit a wide variety of geometrical arrangements of the two constituent phases. In general, the eutectic structure exhibits a regular morphology (fibrous or lamellar) if both phases possess low entropy of fusion, typically, $\Delta S/R < 2$, where S is the entropy of fusion and R is the gas constant [7]. The relative stabilities of the lamellar and fibrous structures have been discussed in detail by Jackson and Hunt [8] and Hillert [9]. When the volume fractions (V_f) of the two eutectic phases are approximately the same ($30\% < V_f < 50\%$), which is encouraged by a phase diagram that is symmetrical about the eutectic composition, there is a preference for the formation of lamellar structures. If the difference in the volume fractions of the two phases is large (i.e. if one of the phases has $V_f > 70\%$), the total interface energy is less for a fibrous morphology than for the lamellar morphology. In such cases, a fibrous structure is preferred with the major phase becoming the continuous matrix and the minor phase the discontinuous rods.

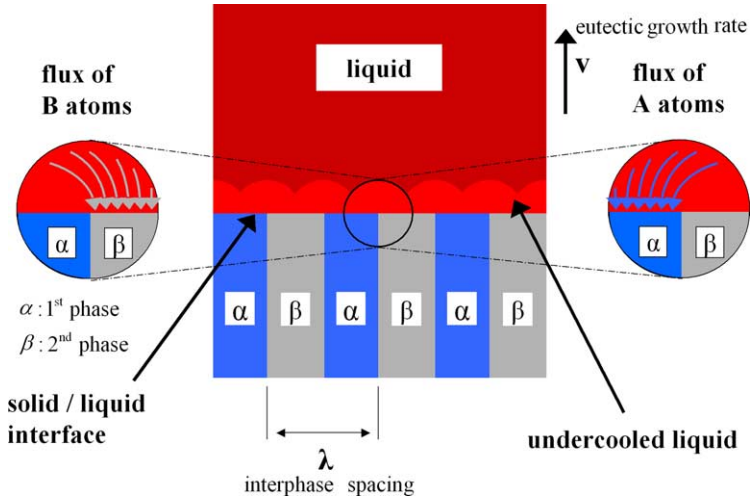

Fig. 1. Schematic of eutectic growth mechanism.

When a pure eutectic alloy is constrained to grow unidirectionally, the two phases in the eutectic colonies grow cooperatively in a direction approximately parallel to the heat flow direction with the solid–liquid interface remaining planar throughout the solidification process. Regular eutectic growth depends on an interplay between the diffusion required for phase separation and the energy required for the formation of interphase boundaries. The interphase spacing is the result of a balance between two competing tendencies:

- on the one hand, to minimize the interphase spacing in order to shorten the diffusion path in the liquid near the interface;
- and on the other hand, to increase the spacing to minimize the interfacial area and hence the total interfacial energy.

The most comprehensive treatment of this balance was established by Jackson and Hunt [8]. Under maximum growth velocity assumptions, they obtained the following relationship between growth rate v and the inter-phase spacing λ, for both lamellar and fibrous eutectic structures:

$$\lambda^2 v = \text{constant} \quad (1)$$

It should be noted that the solidification rate cannot be used to vary the interphase spacing without limit because the well-aligned microstructure breaks down at very low or very high growth rates, being replaced with the so-called degenerate and cellular structures, respectively [10].

The pre-cast NiAl–Re eutectic was directionally solidified as described in Section 2. This nanostructured material was subsequently employed in the experiments of the section below.

3.2. Nanowire production by chemical dissolution of the matrix

The appropriate and selective etching of the NiAl matrix may allow the rhenium fibers to stay, giving a structure in which rhenium nanowires stick parallel to each other in a corroded matrix. The addition of a protective polymer to block any space between the wires, followed by polishing and grinding of the developed structure, would allow the formation of nano disc electrodes, as shown in Fig. 2.

The selective etching of the NiAl phase in the prepared alloy was achieved after digestion of the sample into a solution containing HCl and H_2O_2, as described in Section 2.3. The concentration of both HCl and H_2O_2 used yielded the total oxidation of the NiAl matrix, with the rhenium phase remaining in the solid. ICP-OES analysis of both the solution and the membrane recovered after extraction of the digested sample showed a concentration of Ni and Al which equalled that of the metals in the untreated alloy (30%, w/w for Al and 66%, w/w for Ni). Rhenium, on the other hand, was present in the same solution at lower concentrations, thus only 1.9% (w/w) of rhenium was dissolved, compared to 5.5% (w/w) of the metal present in the eutectic (Table 1). The amount of the three metals extracted in the filtration membrane was negligible, indicating that rhenium has mainly remained in the solid phase. This behaviour can be explained since the

Table 1
Metal contents obtained by ICP-OES for the disintegrated original material and after treatment of the NiAl–Re alloy with HCl/H_2O_2

Sample	Metal content					
	Al		Ni		Re	
	mg/l	%, w/w	mg/l	%, w/w	mg/l	%, w/w
NiAl–Re alloy	–	29.9	–	65.0	–	5.5
Filtered solution[a]	6780	31.2	14550	66.9	420	1.9

[a] Recovered after filtration of the alloy sample treated with HCl/H_2O_2.

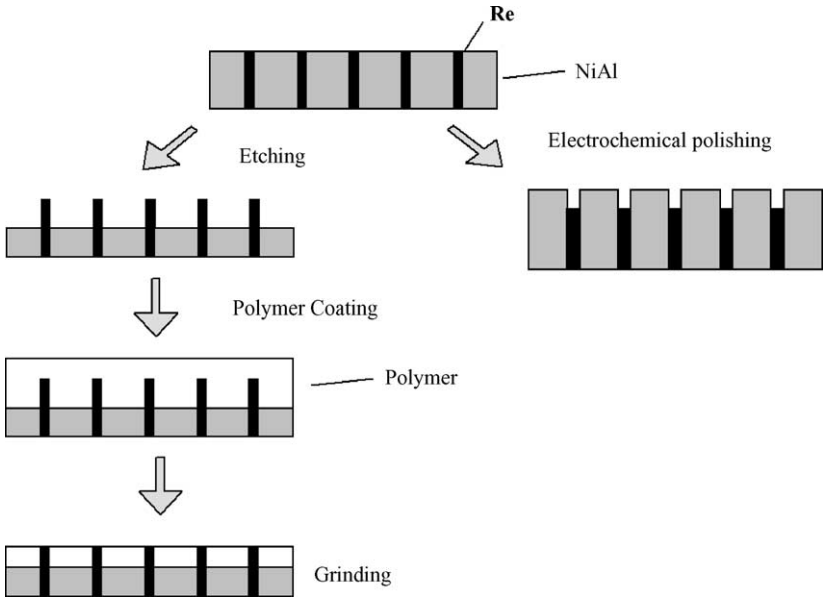

Fig. 2. Schematic of the preparation routes for nanowire arrays and nanopore arrays.

long hair wires are still connected with the base. A different result must be expected if the Re just solidifies in nanoscopic short peaces, which would be washed away after dissolution of a sufficient amount of matrix. They would travel in the solution as colloides and would be intercepted by the filter. These results indicate the suitability of the procedure for the selective etching of the NiAl matrix, and thus the production of Re nanowires.

SEM pictures of the alloy sample taken after digestion in HCl/H_2O_2 showed large fibers embedded in the partly dissolved matrix, with variable length and a diameter of ~400–450 nm, which correlates with the diameter of the Re fibers obtained after solidification in the eutectic cell as predicted from Eq. (1) for the growing speed used (Figs. 3 and 4). The X-ray spectra recorded for these fibers also confirmed that they are composed of rhenium. The Re peaks were dominant and neither Ni nor Al peaks were observed.

3.3. Production of nanopore arrays by electrochemical dissolution of the Re fibres

An alternative route for the fabrication of such nano structures would be the selective dissolution of the minor alloying component, thus yielding nanospaces imbedded into the matrix (Fig. 2). These spaces could then being filled up with metals such as gold for the preparation of alternative nanodisc electrodes. The relation of the chemistry of the phases, however, makes it difficult. On one side, we have the NiAl phase that consists of an equiatomic alloy that will show either the chemistry of the nickel or that of the aluminium dependent on

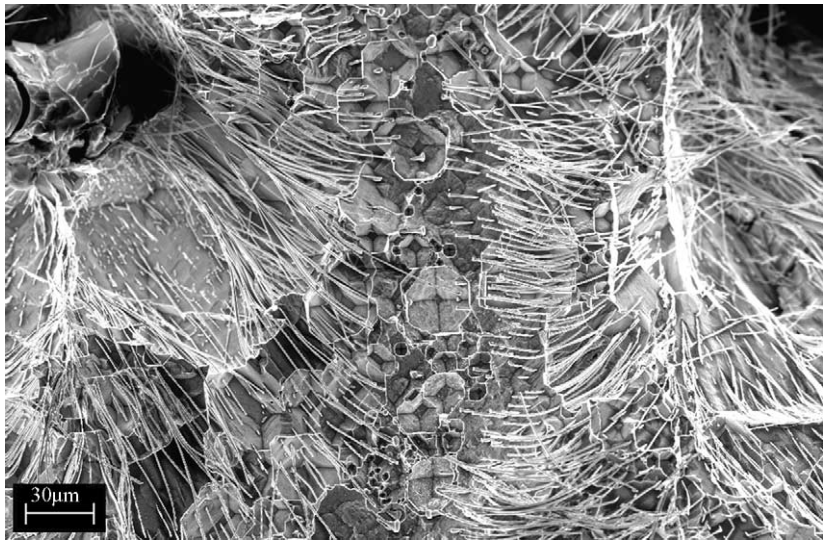

Fig. 3. SEM images of NiAl–Re alloy after digestion in HCl/H_2O_2.

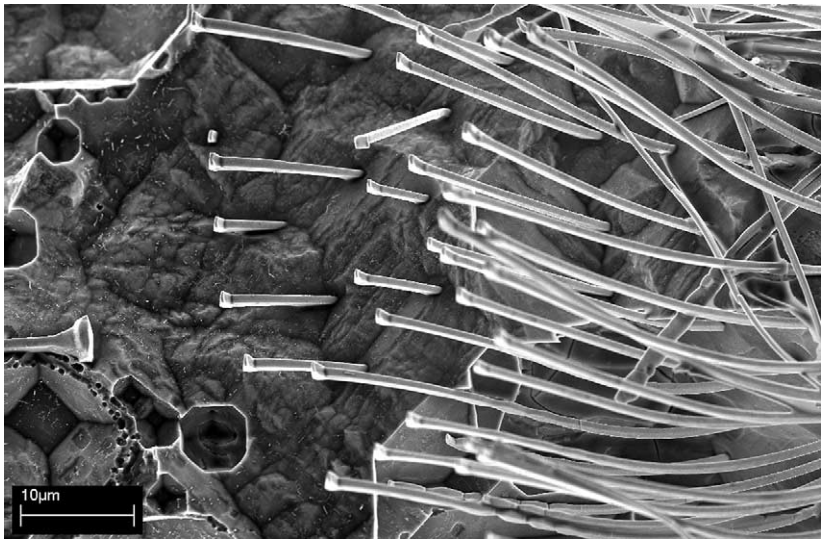

Fig. 4. Re fibers observed in the corroded NiAl matrix after chemical dissolution of the matrix. The aspect ratio, the homogeneous diameter and the parallel assignement are clearly visible.

which of both elements remains during a selective alloy dissolution. Under certain circumstances, the alloy will show its own specific chemistry. The minor phase on the other hand consists of Re which is a refractory metal that can behave similar to a noble metal, but it can also be subject to dissolution. Among all elements, Re has the highest number of possible oxidation states that further complicates a chemical route. Based on the aforementioned, an electrochemical route was chosen. The advantages are:

- mild chemical environments can be employed;
- thermodynamic data is available from the Pourbaix diagram;
- oxidation force can be precisely adjusted by the electrochemical potential;
- reaction rate can be monitored in situ by current measurement.

Beside the thermodynamic aspects, the kinetics of passivation allows to protect the NiAl [11]. The electrochemical anodization of the NiAl–Re alloy leads to the formation of nickel and aluminium oxides, which then create a passive film [12–15], whereas rhenium "dissolves" due to its oxidation to soluble perrhenate [16,17].

The electrochemical behaviour of the NiAl–Re alloy was investigated in an acetate solution (pH 6.0) in order to study the possible passivation of the alloy surface. Cyclic voltammograms recorded in the range from −0.5 to 2.0 V displayed an anodic current which decreased significantly after successive scans (Fig. 5). Such a decrease may be due to the oxidation of the NiAl matrix to create a stable oxide film, which would inhibit or hinder any other process to take place on the electrode surface. It can also indicate the successful dissolution of Re which slows down with deeper digging into the material. SEM pictures like in Fig. 6 of the so anodised sample showed a relatively smooth surface with a high density

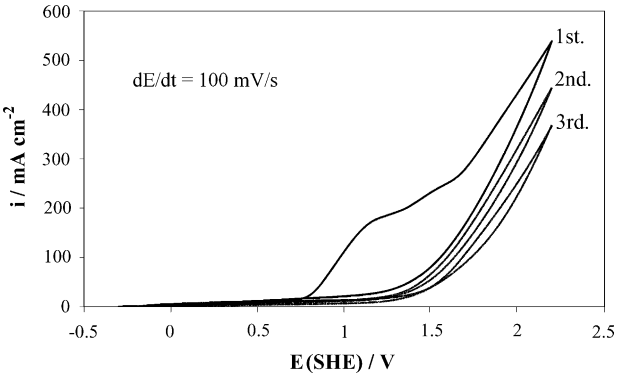

Fig. 5. Cyclic voltammograms consecutively recorded for polished NiAl–Re electrodes in 0.1 M acetate buffer pH 6.0 (scan rate = 100 mV s^{-1}).

of "nanopores" attributed to the dissolution of the rhenium fibers after the oxidation process.

According to the Pourbaix diagrams of the three components involved: Ni, Al and Re, in water at 25° C, at the studying pH (6.0) and potential range (−0.5 to 2 V), the aluminium oxide and nickel oxide should be thermodynamically stable, whereas the rhenium would predominantly be present in the form of soluble perrhenate [18]. This is in good agreement with the experimental observations, which showed dissolution of the rhenium fibers probably due to their oxidation. Al and Ni, on the other hand, formed stable oxides which deposit on the surface and passivate the electrode (Fig. 7).

The different behaviour observed when oxidation was conducted in the presence of HCl is due to pitting corrosion at low pH originated on the oxide films by the aggressive chloride ions [15–17], which would produce Al^{3+} and Ni^{2+} species that are highly soluble in aqueous media. At the low pH provided by the HCl medium, rhenium will only be immune over a small cathodic potential range; this indicates that the maximum potential created by the HCl/H_2O_2 medium falls within

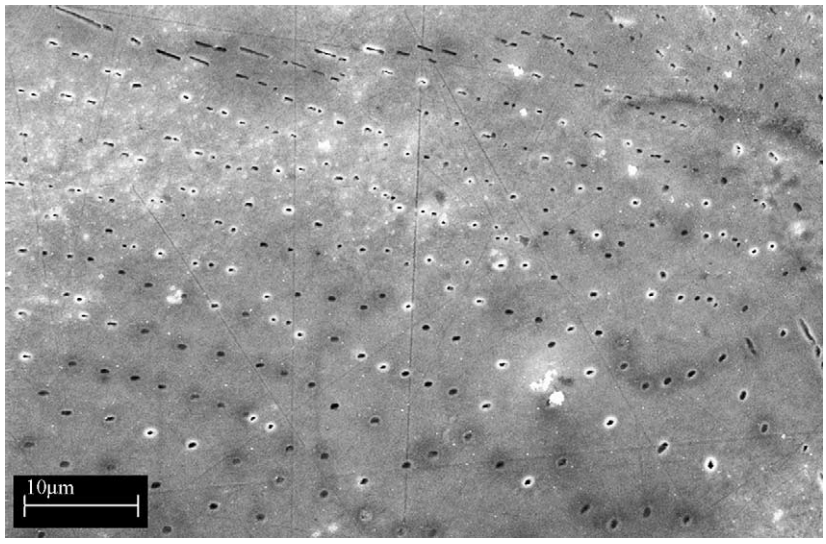

Fig. 6. SEM image of NiAl–Re alloy after electrochemical oxidation at pH 6.0.

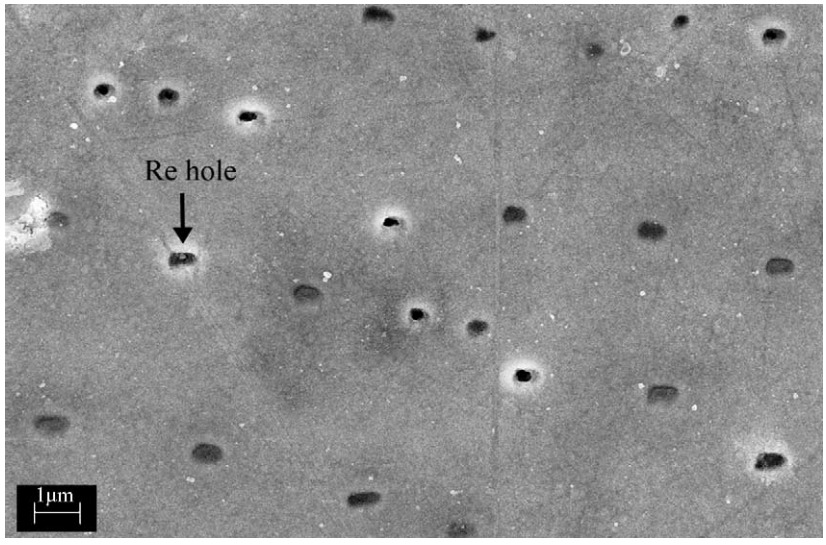

Fig. 7. SEM image of the NiAl–Re alloy after passivation at pH 6.0. The holes present in the structure are attributed to rhenium dissolution to perrhenate.

the stability range. At very acidic pH values the Pourbaix diagram predicts that Al will mainly be present as a cation over a very wide potential range (above −1.7 V), whereas Ni will only be as Ni^{2+} over the −0.3 to 1.8 V range. For rhenium to stay in the metal state, the potential must be close to 0 V. Anodic potential will show rhenium in the form of different oxides (ReO_2, ReO_3) or ReO^{4-}, which would dissolve in the attacking solution.

4. Conclusions

The formation of nanodisc electrodes consisting of arrays of rhenium nanofibers seems feasible after corrosion of the matrix in the presence of chloride ions in highly acidic media. A novel route for the preparation of nanopre arrays in NiAl is presented here. It starts from a directionally solidified eutectic NiAl–Re alloy. The diameter of the fibres and the interfiber spacing was already determined by the growth rate and the temperature gradient of undercooling. The electrochemical process used works in a harmless acetate buffer and selectively electrodissolves the Re.

This process has a high potential in nanotechnology. Most likely, the process will also work with material from different solidification rates to give arrays of smaller pores with smaller λ. The nanostructured material introduced here shall be used to deposit metals-like gold into the pores to give a nanoelectrode array that might prove useful in electrochemical sensors. A continued Re dissolution on the other hand could allow the production of nanofilters for sterile filtration or gas separation.

Acknowledgement

The financial support of the Deutsche-Forschungs-Gemeinschaft through the project Production of Nanowire Arrays through Directional Solidification and their Application within the DFG Priority Programme 1165 Nanowires and Nanotubes—from Controlled Synthesis to Function is gratefully acknowledged.

References

[1] D. Appell, Nature 419 (2002) 553.
[2] Y. Xia, P. Yang, Y. Sun, Y. Wu, B. Mayers, B. Gates, Y. Yin, F. Kim, H. Yan, Adv. Mater. 15 (2003) 353.
[3] S. Iijima, T. Ichihashi, Nature 363 (1993) 603.
[4] Z.L. Wang, J. Phys. Condens. Matter 16 (2004) 829.
[5] H.J. Fan, R. Scholz, D.M. Kolb, M. Zacharias, Appl. Phys. Lett. 85 (2004) 4142.
[6] D. Ma, R. Lentzen, P.R. Sahm, Giessereiforsch 38 (1986) 106.
[7] J.D. Hunt, K.A. Jackson, Trans. Metall. Soc. AIME 236 (1966) 843.
[8] K.A. Jackson, J.D. Hunt, Trans. Metall. Soc. AIME 236 (1966)1129.
[9] E.P. George, H. Bei, K. Serin, G.M. Pharr, Mater. Sci. Forum 426–432 (2003) 4579.
[10] M. Hillert, in: J.L. Walter, M.F. Gigliotti, B.F. Oliver, H. Bibring (Eds.), Proceedings of the Conference on In Situ Composites-III, Ginn Custom Publishing, Lexington, 1978, p. 1.
[11] J.W. Schultze, A.W. Hassel, Passivity of metals, alloys, and semiconductors, in: A.J. Bard, M. Stratmann (Eds.), Encyclopedia of Electrochemistry, in: M. Stratmann, G.S. Frankel (Eds.), Corrosion and Oxide Films, vol. 4, Wiley-VCH, Weinheim, 2003, pp. 188–189, 216–270.
[12] B. MacDougall, M. Cohen, J. Electrochem. Soc. 121 (1974) 1152.
[13] C.V. D'Alkaine, M.A. Santanna, J. Electroanal. Chem. 457 (1998) 5.
[14] W.A. Badawy, F.M. Al-Kharafi, A.S. El-Azab, Corr. Sci. 41 (1999) 709.
[15] S. Gudić, J. Radošević, M. Kliškić, Electrochim. Acta 47 (2002) 3009.
[16] A. Giraudeau, P. Lemoine, M. Gross, Corr. Sci. 13 (1973) 421.
[17] J. Gómez, J.I. Gardiazábal, R. Schrebler, H. Gómez, R. Córdova, J. Electroanal. Chem. 260 (1989) 113.
[18] M. Pourbaix, Atlas of Electrochemical Equilibria in Aqueos Solutions, National Association of Corrosion Engineers, Texas, USA, 1974.